

Characterization of MEMS Resonator Nonlinearities Using the Ringdown Response

Pavel M. Polunin, Yushi Yang, Mark I. Dykman, Thomas W. Kenny, and Steven W. Shaw

Abstract—We present a technique for estimation of the model parameters for a single-mode vibration of symmetric micromechanical resonators, including the coefficients of conservative and dissipative nonlinearities. The nonlinearities result in an amplitude-dependent frequency and a nonexponential decay, which are characterized from the ringdown response. An analysis of the amplitude of the ringdown response allows one to estimate the linear damping constant and the dissipative nonlinearity, and the zero-crossing points in the ringdown measurement can be used for characterization of the linear natural frequency and the Duffing and quintic nonlinearities of the vibrational mode, which arise from a combination of mechanical and electrostatic effects. [2015-0263]

Index Terms—MEMS characterization, ringdown, nonlinear damping, Duffing nonlinearity, quintic nonlinearity.

I. INTRODUCTION

MICROMECHANICAL (MEMS) resonators have been extensively studied and attracted significant attention in both the physics and engineering communities due to their multiple beneficial features including high stability, low power consumption and compatibility with integrated circuits [1]–[4]. Being designed as an alternative to conventional oscillators, such as quartz oscillators, MEMS resonators are applied for time keeping and synchronization purposes [5], [6] as well as for sensing of force [7], mass [8], and electronic and nuclear

spins [9], for example. The necessity of high precision in these applications imposes various performance requirements including high quality factor, low phase noise [10] and large signal-to-noise ratio [11]. In order to satisfy these requirements, MEMS oscillators are frequently operated at large vibration amplitudes, which are typically limited by the onset of nonlinearity. To adequately describe and predict the dynamics of the system operating at amplitudes beyond the linear range, it is useful to have a model that includes coefficients for both conservative Duffing and quintic nonlinearities [12] and nonlinear dissipation [13]–[15].

Parameter estimation in vibrational systems is a challenging problem arising in systems of different size scales [16]–[20]. It is important since it allows one to describe the dynamics of systems of interest using standard models [21]–[23], to understand the fundamental physical mechanisms responsible for certain observed effects [24], [25], and to design systems with desired performance characteristics [26], [27]. While several methods have been developed for nonlinear system identification [28], a common approach for determining the model parameters of MEMS resonators is based on the resonant response of a vibrational mode to a periodic force. In this case, the resonator amplitude and phase are measured as a function of the frequency of the external driving field for a fixed level of the drive amplitude. For systems operating in the linear regime this spectral method provides estimates for the linear resonant frequency and the quality factor [29] from a frequency response. When the resonator is driven into its nonlinear regime, the shape of the frequency response is determined by both conservative [30] and dissipative nonlinearities [1], [14], [15]. As a result, it is necessary to perform several measurements at different forcing amplitudes in order to completely characterize the parameters of the vibrational mode [29], [30], and the precision is limited, particularly where several nonlinear mechanisms are involved.

Here we show that a single ringdown response measurement enables full characterization of a vibrational mode of a micromechanical resonator, including parameters for symmetric conservative and dissipative nonlinearities. In particular, estimates of the linear decay rate and the nonlinear friction coefficient are achieved by analyzing the vibrational amplitude during the ringdown. Additionally, the sequence of zero-crossing points is used in this work for characterization of the linear resonant frequency and the Duffing and quintic nonlinearities that cause an amplitude-dependent frequency. This zero-crossing-based method, as compared with the quadrature analysis presented in [1], is simpler for the post-processing

Manuscript received September 26, 2015; revised January 15, 2016; accepted February 5, 2016. Date of publication February 26, 2016; date of current version March 31, 2016. This work was supported in part by the U.S. Army Research Office within the Michigan State University Group, managed by S. Stanton, under Grant W911NF-12-1-0235; in part by the National Science Foundation through the Directorate for Engineering under Grant 1234067; in part by the Defense Advanced Research Projects Agency through the Program Mesodynamic Architectures, managed by Dr. D. Green, under Grant FA8650-13-1-7301; and in part by the National Science Foundation within the Stanford Nanofabrication Facility through the National Nanotechnology Infrastructure Network for fabrication under Grant ECS-9731293. Subject Editor R. Pratap.

P. M. Polunin is with the Department of Mechanical Engineering, and the Department of Physics and Astronomy, Michigan State University, East Lansing, MI 48823 USA (e-mail: poluninp@msu.edu).

Y. Yang and T. W. Kenny are with the Department of Mechanical Engineering, Stanford University, Stanford, CA 94305 USA (e-mail: ysyang88@stanford.edu; tkenny@stanford.edu).

M. I. Dykman is with the Department of Physics and Astronomy, Michigan State University, East Lansing, MI 48823 USA (e-mail: dykman@pa.msu.edu).

S. W. Shaw is with the Department of Mechanical Engineering, and the Department of Physics and Astronomy, Michigan State University, East Lansing, MI 48823 USA, and also with the Department of Mechanical and Aerospace Engineering, Florida Institute of Technology, Melbourne, FL 32901 USA (e-mail: shawsw@msu.edu).

Color versions of one or more of the figures in this paper are available online at <http://ieeexplore.ieee.org>.

Digital Object Identifier 10.1109/JMEMS.2016.2529296

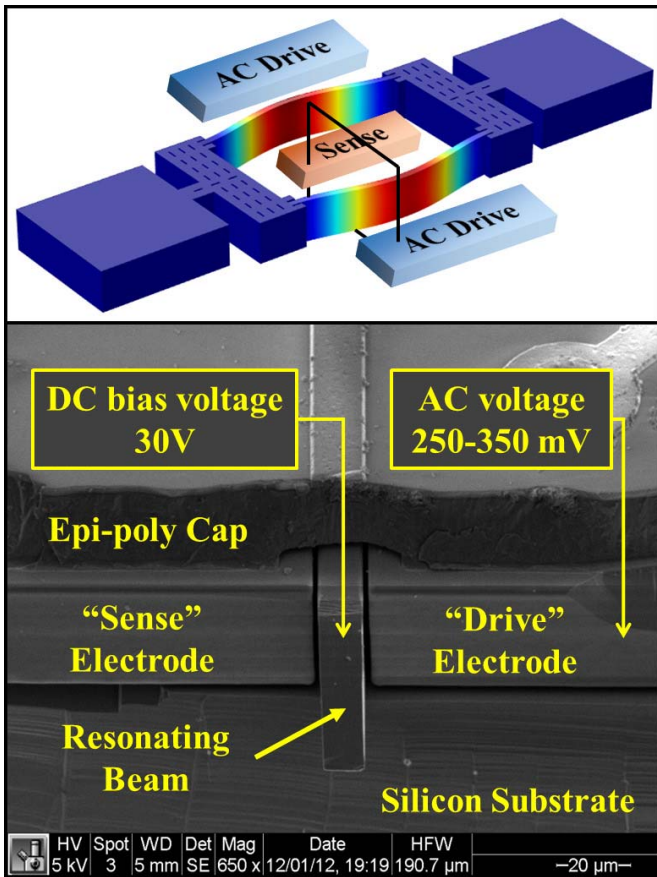


Fig. 1. Top: COMSOL model of a micromechanical DA-DETF resonator showing the symmetric vibrational mode under study. The expected (using FEM analysis) values of the resonator linear parameters in the experiment are as follows: effective mode mass $m_{eff} \sim 0.2 \mu\text{g}$, quality factor $Q \sim 10^3 - 10^4$, and natural frequency $f_0 \approx 1.2 \text{ MHz}$. The square denotes the location of the cross-sectional SEM. Bottom: SEM from a 45° -view angle of the resonator encapsulated with the *epi-seal* process.

and more accurate as it utilizes raw data and does not require additional spectral tools like Fourier analysis. In this work we illustrate the ringdown-based system identification method for characterization of a micromechanical oscillator, but it can be equally successfully applied to nano-scale devices, such as graphene resonators and carbon nanotubes, as well as macro-scale systems. This time-domain characterization method is unique in that its precision does not suffer from noise in the driving electronics, resulting in a model that allows for the prediction of the resonator response in the presence of a driving field or when placed in a feedback loop.

II. RINGDOWN-BASED CHARACTERIZATION METHOD

A. Device Under Study

In this work we carry out the ringdown-based characterization for the double-anchored double-ended-tuning-fork (DA-DETF) resonator shown in Fig. 1. The resonator, which was originally designed for time-keeping applications, was fabricated using an epitaxial polysilicon encapsulation process [31] and it consists of two micromechanical beams $200 \mu\text{m}$ long, $6 \mu\text{m}$ wide and $40 \mu\text{m}$ thick that are connected on both ends to perforated masses, which are further anchored

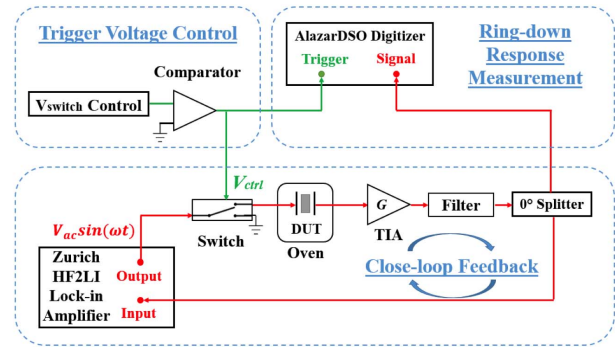


Fig. 2. Variable-phase closed-loop feedback system with added capability for ringdown measurement. The encapsulated devices are placed into a Thermotron S-1.2c environmental chamber for temperature stabilization at -40°C .

to the base. The perforation in the coupling mass serves as release-etch holes and does not affect the device performance. The encapsulation process results in a pressure of $< 1 \text{ Pa}$ in the cavity containing the resonator.

B. Measurement Setup

To prepare the system for the ringdown measurement, we first force the resonator to oscillate in the nonlinear regime using a feedback loop. Previous research has demonstrated stable oscillation of this device beyond the critical bifurcation limit by controlling the operating phase of the resonator when driven in closed-loop [12]. Physically, the feedback loop compensates the losses in the resonator due to damping and provides an additional shift in the resonator phase ensuring that Barkhausen stability criterion is met. In this work, a Zurich HF2LI lock-in amplifier is used to control and maintain a variable-phase feedback loop, as shown in Fig. 2. The output of the lock-in amplifier maintains the resonator motion by supplying a periodic signal ($V_{AC} = 250 - 350 \text{ mV}$) to two “Drive” electrodes. By tuning the phase shift in the feedback loop, we achieve the frequency of self-sustained oscillations to be close to the nonlinear resonance; see Fig. 3. To achieve a strong output signal, we apply a DC voltage ($V_{DC} = 30 \text{ V}$) to the resonator body. Additionally, we maintain both driving and sensing electrodes at this “ground” voltage potential, thus ensuring the symmetry of the system potential energy. Note that a non-zero bias voltage between the resonator body and the attendant electrodes generally affects the conservative forces of MEMS resonators, which we discuss in detail in Section II.C. However, due to the high conductivity of the transmission lines in the measurement setup, we neglect any additional electrostatic damping introduced by the capacitive actuation/sensing scheme.

The resonator response is detected by the “Sense” electrode in the form of current that is electrostatically transduced due to the resonator vibration. This output current is then converted to a voltage signal and amplified via a transimpedance amplifier (TIA). We further pass the signal through a band-pass filter with corner frequencies 1.2 MHz and 7 MHz in order to remove low- and high-frequency measurement noise, and then split the signal with a 0° power splitter.

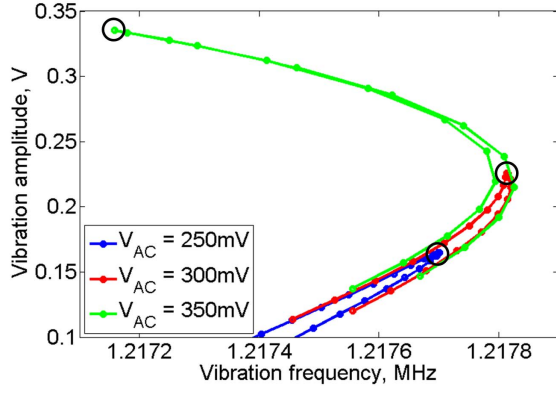


Fig. 3. Measured amplitude-frequency responses of the micromechanical resonator in the feedback loop with $V_{DC} = 30V$ and different values of V_{AC} at $T = -40^\circ C$; the phase step of the closed loop is 5° . Circles denote positions of nonlinear resonance where the system has been prepared for the subsequent ringdown measurement.

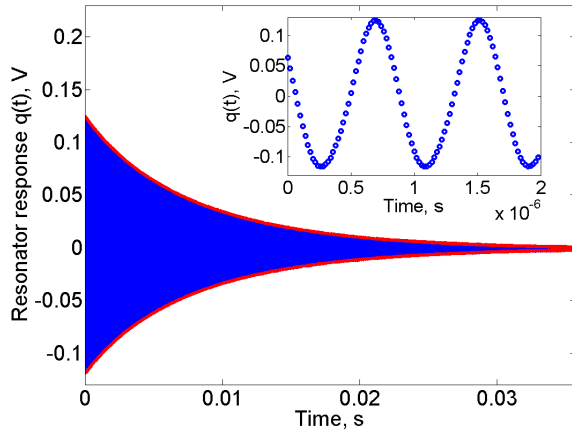


Fig. 4. A measured ringdown response of the resonator under study; $V_{DC} = 30V$ and $V_{AC} = 250mV$. Red solid line indicates extracted vibrational envelope $a(t)$.

One of the outputs is fed back to the lock-in amplifier, where the resonant frequency and amplitude can be tracked. The second signal component goes into an AlazarDSO ATS9360 digitizer for recording the ringdown response. A voltage-controlled RF switch, placed between the lock-in output and the resonator, acts as the mechanism for cutting the resonator driving. When the trigger voltage is set “High”, the connection between the lock-in amplifier and resonator is closed, and we observe stable oscillatory signal via the AlazarDSO. Once the resonator vibrations reach steady-state, the trigger voltage is switched to “Low”. In this case the falling edge cuts the input to the resonator coming from the lock-in amplifier (the transition time constant is $\sim 10^{-6}$ s) and triggers the digitizer, allowing us to capture the full ringdown response, see Fig. 4. The collected data is post-processed for characterization of the parameters of the vibrational mode via the procedure described below.

C. Model

The dynamics of a micromechanical resonator with capacitive sensing depends on both mechanical forces arising in the resonator body and the electrostatic effects due to the bias

voltage [19]. In this work, the resonator flexural displacement $y(x, t)$, where x is the spatial coordinate along the beam, is much smaller than the resonator width, $y(x, t) \ll h$, which allows us to approximate the mechanical restoring force of the symmetric vibrational mode under the study by a 3^{rd} -order polynomial $\omega_{0m}^2 q + \gamma_m q^3$, where q is the modal displacement coordinate, ω_{0m} is the mechanical linear vibration frequency and γ_m is the mechanical Duffing nonlinearity which is positive for a clamped-clamped (CC) beam. These modal parameters can be obtained by approximating the resonator deformation function as $y(x, t) = q(t)\theta(x)$, where $\theta(x)$ is the ideal mode shape of a CC beam. Alternatively, one can use the method of assumed modes, where $\theta(x)$ is given by a simple polynomial that satisfies the CC boundary conditions, for example, $\theta(x) = 16x^2(1-x)^2$, and perform a Galerkin projection of the original equation of motion for the beam onto $\theta(x)$ [19], [32]. Further, since the resonator is biased symmetrically we model the electrostatic force acting on the resonator during its ringdown as $F_{el} = \kappa[(d - y(x, t))^{-2} - (d + y(x, t))^{-2}]$, where d is the nominal electrode gap size and κ is the strength of the electrostatic force, which depends on the resonator dimensions and the bias voltage. In order to obtain the expression for an equivalent electrostatic force acting on the vibrational mode, one would have to project F_{el} on this mode, which is generally a challenging task. However, noticing that, by definition, $y(x, t)/d < 1$, we can expand F_{el} in a Taylor series about $q = 0$. Since $d \ll h$, we can keep in this expansion higher-order terms. These terms can become comparable to the nonlinear term $\propto q^3$ where the expansions of the both mechanical and electrostatic forces apply. We will keep terms up to 5^{th} order in q/d and then perform the Galerkin projection. It is important to note that the mechanical and electrostatic forces are both symmetric. Since the terms of different powers in q can become comparable in these two forces, different effects can come into play depending on the amplitude. The mechanical nonlinearity is hardening and the electrostatic nonlinearity is softening. The natural frequency (from the linear term) includes both effects, and for the present device and bias voltage the cubic term is dominated by mechanical effects and is thus hardening, while the quintic nonlinearity is dominated by the electrostatic effects and is softening. This leads to the inflection point on the amplitude dependence of the vibration frequency seen in Fig. 3.

After combining mechanical and electrostatic effects together, the dynamics of a vibrational mode of a symmetric micromechanical resonator can be described for moderate modal amplitudes ($q \ll d$) by the following phenomenological model

$$\ddot{q} + 2(\Gamma_1 + \Gamma_2 q^2)\dot{q} + q(\omega_0^2 + 2\omega_0\eta(t)) + \gamma q^3 + \beta q^5 = f(t), \quad (1)$$

where q is again the modal displacement coordinate, ω_0 is the natural frequency of the mode, Γ_1 and Γ_2 are the coefficients of linear and nonlinear friction, and γ and β are the coefficients of the conservative Duffing and quintic nonlinearities respectively. The linear damping constant Γ_1 determines the resonator decay at small vibration amplitudes

and is related to the resonator quality factor as $Q = \omega_0/2\Gamma_1$. Note that ω_0 is primarily defined by ω_{0m} , but is slightly reduced by the presence of the electrostatic actuation/sensing scheme (electrostatic frequency tuning effect). To complete the model, we also include additive, $f(t)$, and multiplicative, $\eta(t)$, noise sources, which can be of thermal or non-thermal origin.

Qualitatively, the nonlinear and noise terms in Eq. (1) have the following effects, to first order: the stiffness nonlinearities γ and β cause an amplitude-dependent frequency shift, the nonlinear damping Γ_2 produces an amplitude-dependent damping (and non-exponential decay), while the noise processes make both the amplitude and frequency fluctuate about the deterministic response of the resonator. The decay of the oscillation amplitude is determined by the terms of Eq. (1) proportional to Γ_1 and Γ_2 , and also by $f(t)$ and $\eta(t)$. Thus, in a standard spectral measurement, γ , β and Γ_2 (and the noise terms [25]) lead to a deviation of the spectral contour from the Lorentzian, and it is usually impossible to accurately extract these parameters from a single frequency sweep. In contrast, as we show, a ringdown measurement is very sensitive to these nonlinearities.

In the absence of the noise terms in Eq. (1), the dynamics of the resonator ringdown response can be studied in terms of slowly-varying (on the time scale $\sim \omega_0^{-1}$) resonator amplitude $a(t)$ and phase $\phi(t)$

$$\begin{aligned} \dot{q}(t) &= a(t) \cos(\omega_0 t + \phi(t)), \\ \dot{\phi}(t) &= -\omega_0 a(t) \sin(\omega_0 t + \phi(t)). \end{aligned} \quad (2)$$

Substituting this change of variables into equation Eq. (1), applying the method of averaging, and neglecting fast-oscillating terms [33], we obtain the following equations of motion for the modal amplitude and phase

$$\dot{a} = -(\Gamma_1 + \frac{1}{4}\Gamma_2 a^2)a, \quad (3a)$$

$$\dot{\phi} = \frac{3\gamma}{8\omega_0} a^2 + \frac{5\beta}{16\omega_0} a^4. \quad (3b)$$

From Eq. (3a) it is clear that the amplitude dynamics are unaffected by the conservative nonlinearities, while the phase depends on the amplitude through both γ and β , as expected. In fact, it can be shown that the amplitude decay is independent of γ and β even in the presence of noise [34]. The solution for the resonator vibrational envelope can be obtained in closed form as

$$a(t) = a_0 e^{-\Gamma_1 t / \sqrt{g(t)}}, \quad (4)$$

where $g(t) = 1 + \frac{1}{4}\frac{\Gamma_2}{\Gamma_1} a_0^2 (1 - e^{-2\Gamma_1 t})$ and a_0 is the initial value of the modal amplitude in the ringdown response; see Fig. 4. Using this solution in the expression for $\dot{\phi}$ in Eq. (3b), we obtain the solution for the resonator phase

$$\phi(t) = \frac{3\gamma}{4\omega_0\Gamma_2} \left(1 - \frac{10\beta\Gamma_1}{3\Gamma_2}\right) \ln g(t) + \frac{5\beta a_0^2}{8\omega_0\Gamma_2} \frac{g(t) - e^{-2\Gamma_1 t}}{g(t)}, \quad (5)$$

where we omit the initial resonator phase since it is determined by an arbitrary choice of $t = 0$.

The existence of closed-form solutions for the resonator amplitude and phase allows us to develop a ringdown-based

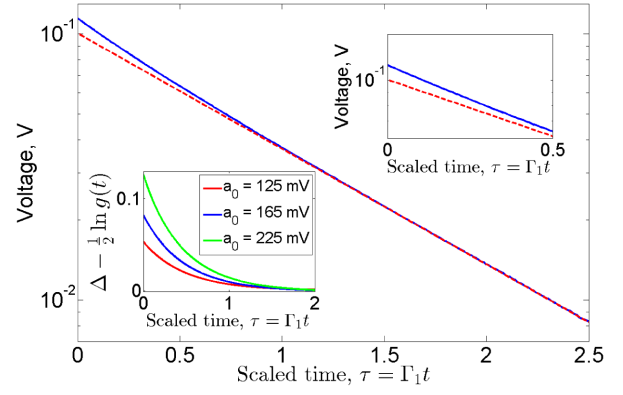


Fig. 5. Measured vibrational amplitude of the DA-DETF resonator during its ringdown response with $V_{DC} = 30V$ (solid line). The dashed line represents the exponential decay of the resonator amplitude at low vibration amplitudes. Upper inset: nonlinear friction causes the ringdown amplitude envelope to deviate from exponential at large amplitudes, which is used for the characterization of Γ_2 . Lower inset: the effect of nonlinear dissipation on the ringdown response becomes stronger as the initial amplitude increases.

technique for estimating the resonator parameters, including conservative and dissipative nonlinear coefficients.

It is worth mentioning a possible origin of the nonlinear dissipation in MEMS resonators. According to the microscopic theory of dissipation discussed in [34], nonlinear friction is an essential consequence of the nonlinear interaction of the primary resonant mode with phonons, as is also the case for linear friction. For high-Q resonators, the adequate description of nonlinear friction is in fact given by Eq. (3a); in the phenomenological picture, the term $\propto \Gamma_2$ can come either from the friction force of the form of $q^2\dot{q}$ or \dot{q}^3 , or from their combination. If the phonons that lead to the relaxation are in thermal equilibrium, there is an interrelation between the nonlinear friction coefficient Γ_2 and the intensity of the noise $\eta(t)$ [14], similar to the familiar interrelation between Γ_1 and the intensity of the additive noise $f(t)$.

D. Characterization Technique and Experimental Results

The shape of the vibrational envelope during the ringdown response, when assumed to obey Eq. (4), differs from a simple exponential form at moderate amplitudes, and the effect becomes stronger as the initial amplitude increases, as shown in Fig. 5. When the resonator rings down, its amplitude decreases and the effect of Γ_2 on the vibrational envelope becomes weaker. In the final part of the ringdown response, the resonator motion is essentially independent of Γ_2 , the resonator energy decays exponentially, and the parameter Γ_1 can be obtained, see Fig. 5. The deviation of the actual ringdown envelope at large amplitudes from the exponential decay characterized by Γ_1 contains the information about the magnitude of the nonlinear damping coefficient. Analysis of equation Eq. (4) shows that the maximum of this deviation (on the logarithmic scale) is $\Delta = \ln\{a_0/[a(t) \exp(\Gamma_1 t)]\}_{t \rightarrow \infty} = (1/2) \ln(1 + \Gamma_2 a_0^2 / 4\Gamma_1)$, which can be used to estimate the magnitude of Γ_2 .

For the analysis, the amplitude-dependent frequency of the recorded ringdown data was shifted down by mixing with the signal at the frequency of the self-sustained oscillations

TABLE I
ESTIMATED VALUES OF LINEAR AND NONLINEAR DISSIPATION COEFFICIENTS AND CONSERVATIVE NONLINEARITIES FOR DIFFERENT INITIAL AMPLITUDES. RINGDOWN MEASUREMENTS HAVE BEEN PERFORMED WITH $V_{DC} = 30V$ AND AT $T = -40^\circ C$

$a_0(mV)$	$\Gamma_1(s^{-1})$	$\Gamma_2(s^{-1}V^{-2})$	$\gamma(s^{-2}V^{-2})$	$\beta(s^{-2}V^{-4})$
125	116.8	7893	1.12×10^{12}	-2.2×10^{13}
165	122.4	8479	0.93×10^{12}	-2.64×10^{13}
225	119	6011	1.05×10^{12}	-2.07×10^{13}

prior to the ringdown, $\omega_{ss} = \omega_0 + \Delta\omega(a_0)$, and passed through a low-pass filter, [1]. Note that frequency ω_{ss} was captured by the lock-in amplifier just before the ringdown. We then construct the filtered quadratures, $q_x(t)$ and $q_y(t)$, and compute the measured resonator amplitude as $a_m(t) = \sqrt{q_x^2(t) + q_y^2(t)}$. The $a_m(t)$ curve is then fitted to the form described in equation Eq. (4) using a least squares fit, from which we estimated coefficients Γ_1 and Γ_2 , see Table I.

According to Eq. (3b) the resonator frequency changes along the ringdown response as $\omega(t) = \omega_0 + (3\gamma/8\omega_0)a^2(t) + (5\beta/16\omega_0)a^4(t)$. This behavior of the vibration frequency corresponds to decay along a backbone curve in the amplitude-frequency space. The effects of β and γ diminish as the resonator enters its linear regime and the modal frequency approaches ω_0 . In order to estimate ω_0 , γ and β from a single ringdown response, we analyze the sequence of the zero-crossing times $\{t_i\}$ in the resonator response, i.e., the points that satisfy $q(t_i) = 0$ [35]. During the resonator ringdown, the vibration amplitude and frequency are not constant, but change smoothly in time (ignoring the effects of noise). Based on this, we partition the ringdown response into N intervals of length $2\pi/\omega_0 \ll \Delta t \ll \Gamma_1^{-1}$. We assume that the vibration amplitude and frequency remain essentially fixed within each interval, but change in a discrete manner from one interval to the next. Of course, the frequency is a smooth function of time; our procedure corresponds to a discretization of this function. In this spirit, we define the vibration period associated with k^{th} time interval as $T_k = 2(t_{k,n_k} - t_{k,1})/(n_k - 1) = 2\pi/\omega_k$, where $t_{k,i}$ is the i^{th} zero-crossing point and n_k is the number of zero-crossing points within the k^{th} interval. Extracted values of the vibration period T_k are shown in Fig. 6 for $N = 50$. As expected, the value of the vibration period at the beginning of the ringdown, T_1 , depends on the initial vibration amplitude a_0 due to amplitude-dependent frequency pulling. As the resonator motion decays, the vibration period changes in a monotonic (for $\gamma\beta > 0$ or if the initial amplitude is below the inflection point) or non-monotonic (for $\gamma\beta < 0$ and the initial amplitude above the inflection point) manner and gradually saturates to T_∞ , from which we estimated the linear resonant frequency to be $f_0 = 1.218$ MHz. After obtaining the vibration period (and frequency) as a function of time, we estimate the resonator Duffing and quintic nonlinearities by fitting the amplitude-dependent frequency shift $\Delta\omega(a)$ to the form described by Eq. (3b) using a least squares method, see Table I. Fig. 6 shows that the expected behavior of the vibration period based on the extracted values of ω_0 , γ and β is in a good

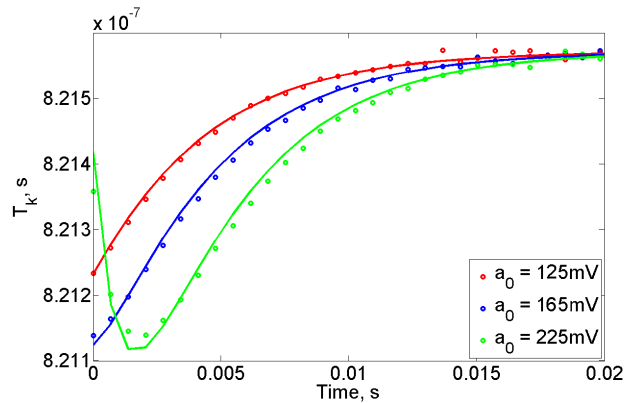


Fig. 6. Vibration period of the resonator during the ringdown as a function of time for different values of initial amplitude. Due to amplitude-dependent frequency pulling, the period varies with time allowing characterization of ω_0 , γ and β from a single measurement. Discrete dots represent extracted values of the vibration period T_k during the ringdown response (error bars $\sim 10^{-11}$ s, not shown). The solid lines represent the expected behavior of the vibration period based on the extracted values of ω_0 , γ and β .

agreement with experimental data. The discrepancy between these two results at large vibration amplitudes is an artifact of the ringdown discretization that was used to obtain T_k . On the other hand, when the resonator amplitude decays, we expect that measurement noise becomes the main source of the discrepancy. In fact, the analysis of the resonator ringdown in Fig. 4 shows that when $q \sim 1$ mV, the resonator response becomes completely random. This observation suggests that the standard deviation of the measurement noise is ~ 1 mV, which justifies the use of the noise-free model for characterization of the resonator parameters.

In this work we have estimated resonator nonlinear dissipative and conservative coefficients with respect to the resonator displacement recorded in units of voltage, see Table I. This representation of the resonator parameters is sufficient for correct modeling of the device dynamics, since Eq. (1) can always be properly scaled using the displacement-to-voltage transduction constant (determined for a particular detection scheme), so that $q(t)$ is expressed in voltage units.

Importantly, the zero-crossing-based method presented here can be easily extended and used to capture the resonator stiffness nonlinearities of orders higher than 5. These higher-order nonlinearities will result in additional terms in Eq. (3b) that dictate the behavior of $\Delta\omega(a)$. Clearly, this method, as compared with analysis using the response quadratures, [1], is accurate and very simple from a computational point of view, as it allows one to extract ω_0 , γ and β directly from the raw data without involving the Fourier transform of a signal that has a non-stationary and, generally, non-monotonic vibration frequency.

III. CONCLUSION

We have shown a method for estimating the deterministic parameters for the symmetric vibrational mode of MEMS resonator using a single ringdown measurement. This is a distinctive feature of this technique as compared to spectral methods, such as the frequency sweep. We have illustrated how to extract values of the linear and nonlinear friction coefficients from the shape of the vibration envelope and the modal natural

frequency and the conservative nonlinearity from the ringdown zero-crossing times. A key to the method is that the vibrational amplitude is affected only by the dissipation parameters, while the frequency and phase are additionally affected by the conservative nonlinearity, thereby uncoupling the characterization process. Another advantage of the characterization method is that the electronics that are responsible for the resonator drive do not affect the ringdown process and, as a result, do not contribute uncertainties to the characterization process. Ongoing work in this area is considering use of the measured fluctuations in the amplitude and the zero-crossing times in order to characterize the additive and multiplicative modal noise processes, and varying the DC bias to distinguish and characterize the mechanical and electrostatic forces.

ACKNOWLEDGMENT

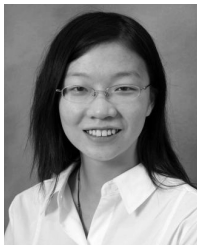
The authors would like to thank the staffs at SNF for their help during the fabrication process.

REFERENCES

- [1] P. Polunin *et al.*, "Characterizing MEMS nonlinearities directly: The ring-down measurements," in *Proc. IEEE 18th Int. Conf. Solid-State Sens. Actuators, Microsyst. (TRANSDUCERS)*, Jun. 2015, pp. 2176–2179.
- [2] C. T.-C. Nguyen, "MEMS technology for timing and frequency control," *IEEE Trans. Ultrason., Ferroelectr., Freq. Control*, vol. 54, no. 2, pp. 251–270, Feb. 2007.
- [3] S. Tabatabaei and A. Partridge, "Silicon MEMS oscillators for high-speed digital systems," *IEEE Micro*, vol. 30, no. 2, pp. 80–89, Mar./Apr. 2010.
- [4] J. T. M. van Beek and R. Puers, "A review of MEMS oscillators for frequency reference and timing applications," *J. Micromech. Microeng.*, vol. 22, no. 1, p. 013001, 2012.
- [5] C. Audoin and B. Guinot, *The Measurement of Time: Time, Frequency and the Atomic Clock*. Cambridge, U.K.: Cambridge Univ. Press, 2001.
- [6] A. Pikovsky, M. Rosenblum, and J. Kurths, *Synchronization: A Universal Concept in Nonlinear Sciences*. Cambridge, U.K.: Cambridge Univ. Press, 2003.
- [7] T. D. Stowe, K. Yasumura, T. W. Kenny, D. Botkin, K. Wago, and D. Rugar, "Attonewton force detection using ultrathin silicon cantilevers," *Appl. Phys. Lett.*, vol. 71, no. 2, pp. 288–290, 1997.
- [8] Y. T. Yang, C. Callegari, X. L. Feng, K. L. Ekinci, and M. L. Roukes, "Zeptogram-scale nanomechanical mass sensing," *Nano Lett.*, vol. 6, no. 4, pp. 583–586, 2006.
- [9] D. Rugar, R. Budakian, H. J. Mamin, and B. W. Chui, "Single spin detection by magnetic resonance force microscopy," *Nature*, vol. 430, no. 6997, pp. 329–332, 2004.
- [10] V. Kaajakari, T. Mattila, A. Oja, J. Kiihamaki, and H. Seppa, "Square-extensional mode single-crystal silicon micromechanical resonator for low-phase-noise oscillator applications," *IEEE Electron Device Lett.*, vol. 25, no. 4, pp. 173–175, Apr. 2004.
- [11] M. Agarwal *et al.*, "Scaling of amplitude-frequency-dependence nonlinearities in electrostatically transduced microresonators," *J. Appl. Phys.*, vol. 102, no. 7, p. 074903, 2007.
- [12] H. K. Lee, R. Melamud, S. Chandorkar, J. Salvia, S. Yoneoka, and T. W. Kenny, "Stable operation of MEMS oscillators far above the critical vibration amplitude in the nonlinear regime," *J. Microelectromech. Syst.*, vol. 20, no. 6, pp. 1228–1230, 2011.
- [13] A. Eichler, J. Moser, J. Chaste, M. Zdrojek, I. Wilson-Rae, and A. Bachtold, "Nonlinear damping in mechanical resonators made from carbon nanotubes and graphene," *Nature Nanotechnol.*, vol. 6, no. 6, pp. 339–342, 2011.
- [14] M. I. Dykman and M. A. Krivoglaз, "Spectral distribution of nonlinear oscillators with nonlinear friction due to a medium," *Phys. Status Solidi B*, vol. 68, no. 1, pp. 111–123, 1975.
- [15] S. Zaitsev, O. Shtempluck, E. Buks, and O. Gottlieb, "Nonlinear damping in a micromechanical oscillator," *Nonlinear Dyn.*, vol. 67, no. 1, pp. 859–883, 2012.
- [16] H. S. Y. Chan, Z. Xu, and W. L. Huang, "Estimation of nonlinear damping coefficients from large-amplitude ship rolling motions," *Appl. Ocean Res.*, vol. 17, no. 4, pp. 217–224, 1995.
- [17] L. Gaul and J. Lenz, "Nonlinear dynamics of structures assembled by bolted joints," *Acta Mech.*, vol. 125, nos. 1–4, pp. 169–181, 1997.
- [18] J. L. Trueba, J. Rams, and M. A. Sanjuán, "Analytical estimates of the effect of nonlinear damping in some nonlinear oscillators," *Int. J. Bifurcation Chaos*, vol. 10, no. 9, pp. 2257–2267, 2000.
- [19] R. Lifshitz and M. C. Cross, "Nonlinear dynamics of nanomechanical and micromechanical resonators," in *Reviews of Nonlinear Dynamics and Complexity*, vol. 1. Hoboken, NJ, USA: Wiley, 2008, pp. 1–52.
- [20] N. J. Miller, P. M. Polunin, M. I. Dykman, and S. W. Shaw, "The balanced dynamical bridge: Detection and sensitivity to parameter shifts and non-Gaussian noise," in *Proc. ASME Int. Design Eng. Tech. Conf. Comput. Inf. Eng.*, 2012, pp. 487–496.
- [21] J. P. Baltanás, J. L. Trueba, and M. A. Sanjuán, "Energy dissipation in a nonlinearly damped duffing oscillator," *Phys. D, Nonlinear Phenomena*, vol. 159, nos. 1–2, pp. 22–34, 2001.
- [22] J. F. Rhoads, S. W. Shaw, and K. L. Turner, "Nonlinear dynamics and its applications in micro- and nanoresonators," *J. Dyn. Syst., Meas., Control*, vol. 132, no. 3, p. 034001, 2010.
- [23] Y. Yang *et al.*, "Experimental investigation on mode coupling of bulk mode silicon MEMS resonators," in *Proc. 28th IEEE Int. Conf. Micro Electro Mech. Syst. (MEMS)*, Jan. 2015, pp. 1008–1011.
- [24] A. Croy, D. Midtvedt, A. Isacsson, and J. M. Kinaret, "Nonlinear damping in graphene resonators," *Phys. Rev. B*, vol. 86, no. 23, p. 235435, 2012.
- [25] Y. Zhang, J. Moser, J. Güttinger, A. Bachtold, and M. I. Dykman, "Interplay of driving and frequency noise in the spectra of vibrational systems," *Phys. Rev. Lett.*, vol. 113, no. 25, p. 255502, 2014.
- [26] E. Buks and B. Yurke, "Mass detection with a nonlinear nanomechanical resonator," *Phys. Rev. E*, vol. 74, no. 4, p. 046619, Oct. 2006.
- [27] M. Bagheri, M. Poot, M. Li, W. P. H. Pernice, and H. X. Tang, "Dynamic manipulation of nanomechanical resonators in the high-amplitude regime and non-volatile mechanical memory operation," *Nature Nanotechnol.*, vol. 6, no. 11, pp. 726–732, 2011.
- [28] G. Kerschen, K. Worden, A. F. Vakakis, and J.-C. Golinval, "Past, present and future of nonlinear system identification in structural dynamics," *Mech. Syst. Signal Process.*, vol. 20, no. 3, pp. 505–592, 2006.
- [29] B. Kim *et al.*, "Temperature dependence of quality factor in MEMS resonators," *J. Microelectromech. Syst.*, vol. 17, no. 3, pp. 755–766, 2008.
- [30] V. Kaajakari, T. Mattila, A. Lipsanen, and A. Oja, "Nonlinear mechanical effects in silicon longitudinal mode beam resonators," *Sens. Actuators A, Phys.*, vol. 120, no. 1, pp. 64–70, 2005.
- [31] R. N. Candler *et al.*, "Long-term and accelerated life testing of a novel single-wafer vacuum encapsulation for MEMS resonators," *J. Microelectromech. Syst.*, vol. 15, no. 6, pp. 1446–1456, Dec. 2006.
- [32] A. N. Cleland, *Foundations of Nanomechanics: From Solid-State Theory to Device Applications*. New York, NY, USA: Springer, 2013.
- [33] N. N. Bogolyubov and Y. A. Mitropolskii, *Asymptotic Methods in the Theory of Non-Linear Oscillations*, vol. 10. Boca Raton, FL, USA: CRC Press, 1961.
- [34] M. I. Dykman and M. A. Krivoglaз, "Theory of nonlinear oscillator interacting with a medium," *Phys. Rev.*, vol. 5, pp. 265–442, 1984.
- [35] A. Demir, A. Mehrotra, and J. Roychowdhury, "Phase noise in oscillators: A unifying theory and numerical methods for characterization," *IEEE Trans. Circuits Syst. I, Fundam. Theory Appl.*, vol. 47, no. 5, pp. 655–674, May 2000.



Pavel M. Polunin received the B.S. degree in automation from Bauman Moscow State Technical University, Moscow, Russia, in 2009, and the M.S. degree in mechanical engineering from Michigan State University, East Lansing, MI, USA, in 2013, where he is currently pursuing the Ph.D. degree with the Department of Mechanical Engineering, and the Department of Physics and Astronomy. His research interests include nonlinear dynamics of MEMS resonators and sensors, noisy systems, reduced order analysis, system modeling, and parameter characterization from design and experiments.



Yushi Yang received the Bachelor's degree in mechanical engineering from Purdue University, West Lafayette, IN, USA, and Shanghai Jiao Tong University, Shanghai, China, in 2011, and the M.S. degree in mechanical engineering from Stanford University, Stanford, CA, USA, in 2013, where she is currently pursuing the Ph.D. degree with the Department of Mechanical Engineering. Her research interests include studying the nonlinear behavior of bulk-mode MEMS resonators, and analyzing the phase noise performance of MEMS oscillators under large driving conditions.

oscillators under large driving conditions.



Mark I. Dykman received the M.S. degree from Kiev State University in 1972; the Ph.D. degree from the Institute of Metal Physics, Ukrainian Academy of Science, in 1973; and the Higher Doctorate degree from the Institute of Semiconductors, Ukrainian Academy of Science, in 1984, all in physics. He was at the Institute of Semiconductors, Kiev, from 1972 to 1991, and Stanford University from 1992 to 1994, and has been with Michigan State University since 1995. He has held visiting appointments as a Professor of Physics at Lancaster University, U.K.;

was an EPSRC Visiting Research Fellow, U.K.; and a Visiting Scholar with the NASA Exploration Systems Directorate. He is a Professor of Physics with Michigan State University. His major areas of interest include condensed matter physics, nonlinear dynamics, transport phenomena, statistical physics far from thermal equilibrium, and quantum computing. He serves on the Editorial Board of *Fluctuations and Noise Letters*. He is a Fellow of the American Physical Society.



Thomas W. Kenny received the B.S. degree from the University of Minnesota, Minneapolis, MN, USA, in 1983, and the M.S. and Ph.D. degrees from the University of California at Berkeley, Berkeley, CA, USA, in 1987 and 1989, respectively, all in physics. From 1989 to 1993, he was with the Jet Propulsion Laboratory, National Aeronautics and Space Administration, Pasadena, CA, where his research focused on the development of electron-tunneling high-resolution microsensors. In 1994, he joined the Department of Mechanical Engineering,

Stanford University, Stanford, CA, where he directs microsensor-based research in a variety of areas, including resonators, wafer-scale packaging, cantilever beam force sensors, microfluidics, and novel fabrication techniques for micromechanical structures. He is the Founder and CTO of Cooligy Inc., Mountain View, CA, (currently, a Division of Emerson), a microfluidics chip cooling component manufacturer, and is the Founder and a Board Member of SiTime Corporation, Sunnyvale, CA, a developer of timing references using MEMS resonators. He is currently a Bosch Faculty Development Scholar and was the General Chairman of the 2006 Hilton Head Solid-State Sensor, Actuator, and Microsystems Workshop, and will be the General Chair of the upcoming Transducers 2015 meeting in Anchorage, AK, USA. From 2006 to 2010, he was on leave to serve as a Program Manager at the Microsystems Technology Office, Defense Advanced Research Projects Agency, Arlington, VA, USA, starting and managing programs in thermal management, nanomanufacturing, and manipulation of Casimir forces, and received the Young Faculty Award. He has authored or co-authored over 250 scientific papers, and holds 50 issued patents.



Steven W. Shaw received the B.A. degree in physics and the M.S.E. degree in applied mechanics from the University of Michigan in 1978 and 1979, respectively, and the Ph.D. degree in theoretical and applied mechanics from Cornell University in 1983. He is a University Distinguished Professor with the Department of Mechanical Engineering, and an Adjunct Professor of Physics and Astronomy with Michigan State University. He has held visiting appointments with Cornell University, the University of Michigan, Caltech, the University of Minnesota,

the University of California–Santa Barbara, and McGill University. His research interests include micro/nanoscale resonators for sensing and signal processing applications, and nonlinear vibration absorbers for automotive applications. He currently serves as an Associate Editor of the *SIAM Journal on Applied Dynamical Systems and Nonlinear Dynamics*. He is a Fellow of ASME, and recipient of the SAE Arch T. Colwell Merit Award, the Henry Ford Customer Satisfaction Award, the ASME Henry Hess Award, and the ASME N. O. Myklestad Award.